ISIJ International, Vol. 44 (2004), No. 12, pp. 1981–1990

Analysis of the Transition State of the Carbon and Iron Oxide Mixture Activated by Mechanical Milling

Yoshiaki KASHIWAYA and Kuniyoshi ISHII

Graduate School of Engineering, Hokkaido University, Sapporo 060-8628 Japan. E-mail: Yoshiaki@eng.hokudai.ac.jp

(*Received on May 24, 2004; accepted in final form on July 8, 2004*)

In previous study, the extremely high reaction rate obtained by the mechanical milling has been reported. It was found that the phenomena were quite complicated and the many factors were affected on the reactivity. Among these factors, the crystal state of hematite and atmosphere (air and argon) during the milling were quite important ones.

Milling of hematite and graphite mixture was carried out both in the air and in the argon. Rate constants for the reactions were obtained by kinetic analysis. The enthalpy ΔH^* and entropy ΔS^* of activation were estimated on the basis of transition state theory. The interpretation of ΔS^* and ΔH^* was performed to explain the effect of milling on the reactivity related to the milling conditions.

The temperature of peak of reaction curve decreased with increasing milling time. The reactivity of the sample milled in the argon atmosphere showed higher reactivity than that milled in the air. The enthalpy ΔH^* and entropy ΔS^* of activation were obtained from experimental rate constants. The variation of ΔH^* and ΔS^* with milling time showed opposite tendency between the sample milled in the air and in the argon. It was considered that the active complex having loose bonding would form during milling in the air atmosphere. On the other hand, the active complex having a structure closed to the product (metallic iron) might form.

KEY WORDS: mechanical milling; active complex; entropy of activation; enthalpy of activation; transition state; iron oxide; graphite.

1. Introduction

In Japan, about 100 million tons iron are produced every year. The energy for the production of iron is significantly large and about 12% to the total energy consumption in Japan. Most of pig iron is made by Blast Furnace in Japan. In the view points of the productivity and the energy efficiency for the reactor of iron production, blast furnace has highest ones. However, such a blast furnace has further possibility for the increase of the efficiency in accordance with the high reaction rate and the low reaction temperature, because the theoretical utilization of CO gas and input energy has some allowance for the improvement.

In the Project of 'the innovational ironmaking reaction in new blast furnace at half energy consumption and minimum environmental influences' (from 1999 to 2004, Chaired by Prof. Ishii, Hokkaido University), many researchers in the ironmaking field have performed their investigations, in which they were classified into 4 groups: (1) Study on the high rate reduction and gasification, (2) Study on the optimization of the structure and composition of iron ore and coal, (3) Study on the lowering of the temperature of melting of metallic iron and slag, (4) Study on the establishment of process image and the quantification of influence of new ironmaking process).

In present study, the authors were belonging to the research group (1) on the high reduction rate and clarification of the mechanism of coupling reaction. We have conducted the study on the coupling phenomenon in previous paper.[1)]

Recently, it was reported that the iron ore–carbon composite pellet has a high reaction rate and a low reaction temperature. To make clarify the mechanism of the reaction in the iron ore–carbon composite, it could obtain a key to a breakthrough for the higher reaction rate and the lower reaction temperature.

From the results of previous study[1,2)] in our laboratory, it was found that the complicated phenomena existed in the system depending on the location and the distance between iron oxide and graphite.

From the contact to the separate situation, there will be many states of the contact between carbon and iron oxide. We clasify those three levels as follows.

I: A separate situation between iron oxide and carbon (**Fig. 1**)

II: A weak contact situation between iron oxide and carbon (**Fig. 2**)

III: A strong contact situation between iron oxide and carbon introduced by mechanical milling (**Fig. 3**)

• In the case of I, it is a separate situation between iron oxide and carbon. The direct reduction by the solid carbon never occur, apparent direct reduction, that is, the indirect reduction by CO gas and carbon gasification reaction will be dominant.

• In the case of II, it could be explained as a weak contact

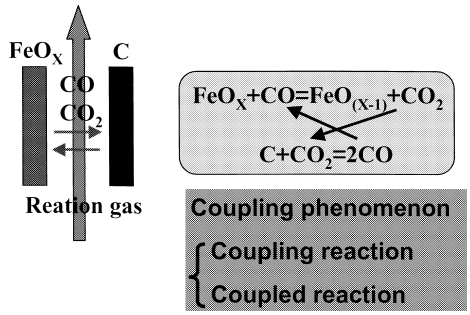

Fig. 1. A separate situation between iron oxide and carbon.

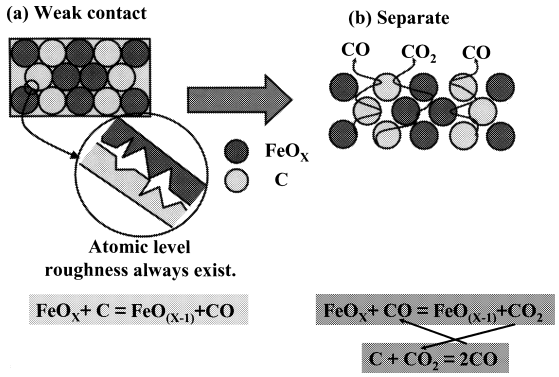

Fig. 2. A weak contact situation between iron oxide and carbon.

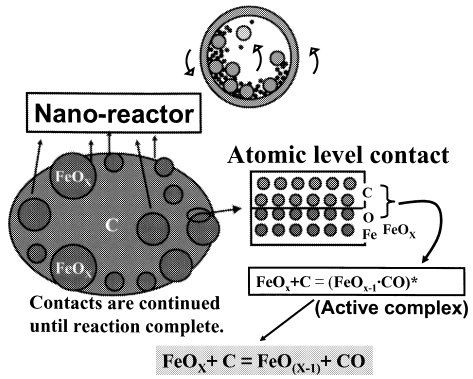

Fig. 3. A strong contact situation between iron oxide and carbon introduced by mechanical milling.

situation, where not only the atomic level roughness but also the macroscopic level one always exist (Fig. 2), because the two reactants (iron oxide and carbon) are just mixed without any pressure. Even if the iron oxide and carbon are contacting at the beginning of reaction, the interface will soon separate, in which the coupling phenomenon (Case I) will be dominant.

It could be considered that the ultimate contact would be the distance that the both reactant atoms were closed to the position where the reaction easily occurred (activated complex). However, until this distance, the variety of distance would exist according to the preparing condition. Actually, the contact situation between iron oxide and carbon would be different from the way of mixing.

In addition to the microscopic feature, the macroscopic feature is important and will affect the apparent reaction rate strongly. Most important nature would be the separation of the both reactants during reaction, which means that the reaction mechanism would be changed in the course of reaction. From these considerations, the reaction rate would show the stable value and could be changed strongly in accordance with the condition of the contact. The mechanical milling is one of the method which can introduce the variety of contact situation into the carbon and iron oxide mixture from the various milling conditions, that is, many kind of activated complex can be formed.

- In the case of III, a strong contact situation between iron oxide and carbon introduced by mechanical milling is illustrated in Fig. 3. In previous study,[1] the milling of hematite and graphite mixture in long time (around 100 h) could give a quite high reaction rate and low reaction temperature. In such a situation, the nano-reactor was constructed in the sample. Especially, the structure of nano-reactor was important and took the situation that the nano-size hematite intruding into the graphite particle as shown in Fig. 3. By the nano-reactor having this structure, the reaction reduction could continue until the reaction completion. And contact mode between carbon and iron oxide is very strong and it could be explain as the activated state, which means the activated complex.

In this study, to clarify the mechanism of the reaction of iron oxide and carbon mixture made by the mechanical milling, the analysis of rate constants obtained in previous study was performed.[1] From the view point of the formation of activated complex introduced by mechanical milling, the enthalpy and entropy of activation were derived and the discussion was carried out on the structure of the activated complex. Furthermore, the changing of reaction mechanism was explained in accordance with the difference of milling atmosphere.

2. Experimental

The details of experiment were shown in previous paper.[1] Here, outline of the experiment is briefly shown. Several kind of hematite samples were prepare (details was shown in below) and high purity graphite with high density (1.77 g/cm^3) and low ash content ($<$100 ppm)) were used as starting materials. Reactivity of the milled sample was studied by TG-DTA (sample weight: 20 mg, resolution: 1 μg). The crucible was made of platinum and 4 mm in inner diameter and 3 mm in depth. The mixture of hematite and graphite with a fixed composition (19.84 mass% C in hematite, which corresponds to C/O$=$1.1) was subjected to ball milling and the milling time was varied from 6 to 100 h. The milling experiment was performed using a planetary ball mill. A ceramics (Alumina) vessel of 500 cm^3 volume, charged with 10 alumina balls of a nominal diameter of 20 mm, was used as the milling medium in all the experiments. The rotating speed of the vessel was maintained constant at 200 rpm for revolution. TG-DTA experiments were conducted under an Ar atmosphere with a constant flow rate of 50 Ncc/min. Samples were heating up with a constant heating rate of 10 K/min from room temperature up to 1 373 K and kept at this temperature for 1 800 s.

2.1. Difference of Sample as a Starting Material and Milling Condition

Since the difference of the particle morphology and crys-

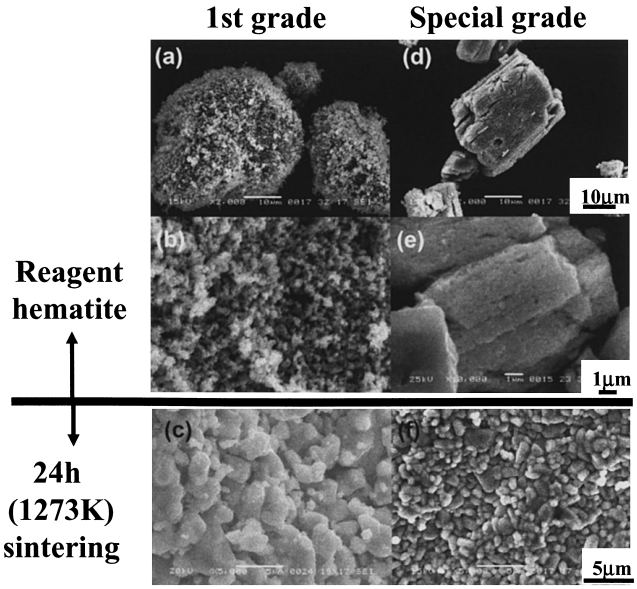

Fig. 4. SEM observation of reagent and sintered hematite particles.

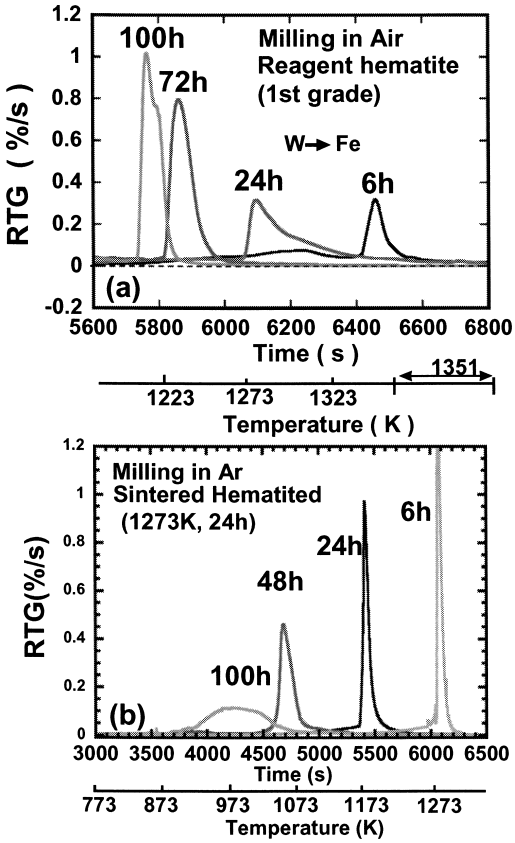

Fig. 5. Comparison of reaction curves between the samples milled in the air and in the argon. (a) Reagent hematite, air atmosphere, wustite-iron reduction; W–Fe, (b) sintered hematite, argon atmosphere, magnetite–iron reduction: M–Fe.

tal structure of sample as a starting material affect strongly on the result of milling, several kind of hematite was prepared. Even a reagent grade hematite (1st grade (>99%) and special grade (>99.99)) have a different type of particle morphology as shown in **Fig. 4**. Moreover, the sample sintered at 1 273 K, 24 h has shown the different grain size between 1st grade and special grade hematite (Figs. 4(c) and 4(f)). A crystalline size of 1st grade reagent sample sintered at 1 273 K, 24 h was larger than that of special grade, and the range of crystalline size for 1st grade was from 1 to 5 μm and special grade hematite was from 1 to 2 μm. In the present experiment, only one kind of graphite was used for making clear the effect of hematite condition.

The atmosphere during milling was also very important factor affecting on the reactivity of the milled sample. In the case of air atmosphere, when the hematite crystal was broken during milling, the active new surface will react with oxygen quickly. If there was no oxygen in the atmosphere (argon atmosphere), the active surface will react with the active carbon (the milled carbon became also active), which meant the direct reduction between iron oxide and carbon (the detail mechanism was discussed below). Actually, we detected the CO gas evolution and the formation of FeO. The details will be published in the same journal.[4,5] Therefore, the inert (argon) atmosphere and the air atmosphere were selected for the milling of different type of hematite.

3. Results and Discussions

3.1. Classification of Phenomena

As mentioned above, crystal conditions (reagent or sintered hematite) and milling atmosphere (argon and air) are very important factors. The experiments were carried out with samples prepared by those combinations. **Figure 5** shows the results of the reactivity measurement experiment of the sample milled under the different conditions. Figure 5(a) shows the comparison of wustite reduction (W–Fe) curves (RTG means the rate of reaction which were obtained by the differential of TG curve (weight loss curve)),[1] in which the reagent hematite (1st grade) was used without any treatment and the atmosphere during milling was an air. The temperature at the peak of RTG curve decreased with the increasing milling time. Furthermore, the maximum value of the curve increased with the milling time.

On the other hand, when the hematite (1st grade) was sintered at 1 273 K for 24 h (Fig. 5(b)), only 6 h milling could attain almost the same reaction rate (RTG was about 1.2%/s) as the 100 h milling (RTG=1.0%/s, Fig. 5(a)) for the reagent grade hematite under an air atmosphere. The peak temperature of the reaction curve decreased furthermore from 1 277 K (6 h) to 983 K (100 h). From these results, it was found that the hematite sintered at 1 273 K showed higher reactivity after milling. The sintered sample was also milled in air atmosphere (the results were not shown in present paper), the reactivity was higher than that of reagent grade hematite, but slightly lower than that of sintered hematite milled under argon.

Figure 6 shows the comparison of RTG curves of H–M, and M–W reduction curves between the reagent hematite in air and the sintered hematite in argon, which both the samples were milled in 100 h. It was quite interesting that the H–M and M–W reduction curves were disappear in the sintered hematite (Fig. 6(b)). The H–M reduction never showed the peak and the easy monotonous slope until 11.5% of reduction degree was observed in every sintered samples. This tendency of reduction curve means almost

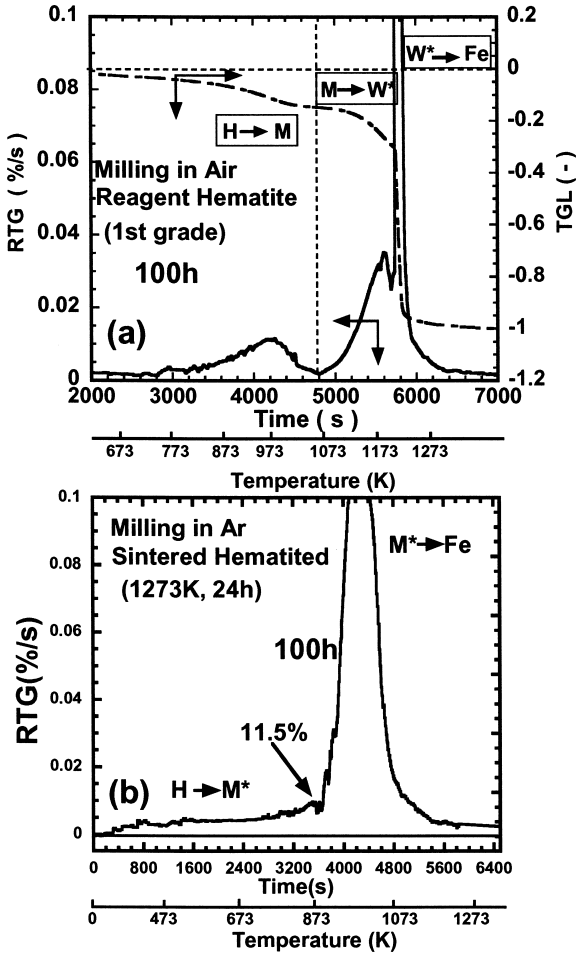

Fig. 6. Typical reaction curves for the H–M and M–W reduction in the different milling conditions.

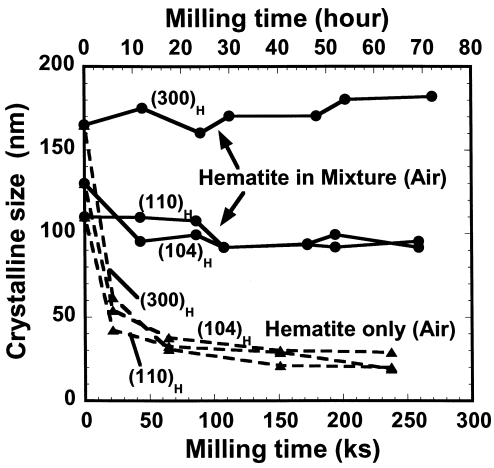

Fig. 7. Variation of crystalline size of hematite with the milling time (hematite and graphite mixture and hematite only in the air).

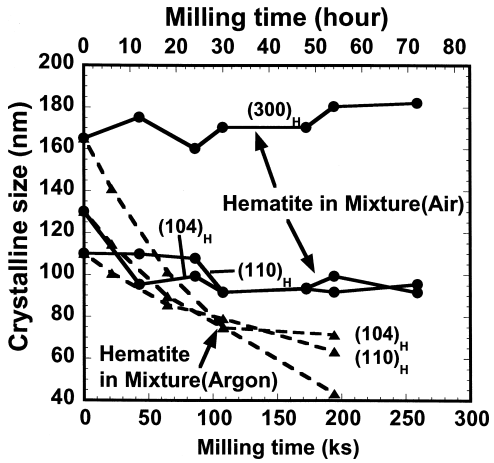

Fig. 8. Variation of crystalline size of hematite with the milling time (hematite and graphite mixture in the air and in the argon).

constant value of the rate constant and is close to the zero order reaction. It might be resulted from a disordered hematite structure by the milling. It would suggest that the sintered hematite was easier to break than the reagent hematite.

As it was considered that the crystalline size after milling affected strongly on the reactivity of sample, X-ray diffraction (XRD) was carried out and crystalline size was estimated using Scherrer's equation.[3] Here, we should note that the particle size and the crystalline size were not always equal. If the original crystalline size was large and equal to particle size, the decreasing mode between the particle and the crystal would be same. However, as shown in Figs. 4(b) and 4(e), the particle was constructed with smaller crystal (polycrystal), the way of decreasing would be different from the kind of reagent grade hematite. On the other hand, the sintered hematite has larger particle size from 1 to 2 μm for special grade hematite and 1 to 5 μm for 1st grade hematite. Since the crystalline size obtained by XRD is different from the particle size, it should be taken into account the difference of particle crystallinity. **Figure 7** shows the variations of crystalline size of sintered hematite according to the milling, which were measured using the different peak of XRD for hematite (in Fig. 7, typical results obtained by (300), (110) and (104) were shown). It was found that the size of crystal was different from orientation and the size in the [300] direction was larger than that in the [110] and [104] directions. Although the particle size of sintered hematite was 1 to 5 μm as mentioned above, the crystalline size measured by XRD was from 100 to 180 nm which were almost the same as the original size of crystal before sintering. According to milling condition, the way of decreasing of crystalline size was different. In the case of milling of hematite–carbon mixture under air condition, the size of hematite crystal was almost the same in spite of long time milling. While the milling of the sintered hematite alone under air, crystalline size quickly decreased within 24 h. The final size of crystal for only the hematite milling was about 30 nm and the difference among different planes was smaller than that of milling of mixture in air. These results would related to the reduction reaction and the reoxidation during milling (the details was mentioned below).

Figure 8 shows the comparison of crystalline size of sintered hematite in mixture under argon atmosphere with the one under air atmosphere. In the case of argon atmosphere, the crystalline size decreased with the increasing milling time. From the result of gas analysis, it was found that the CO gas evolution occurred during the milling under the argon atmosphere,[4] which meant the reduction reaction occurred during milling. This result also suggested that the re-

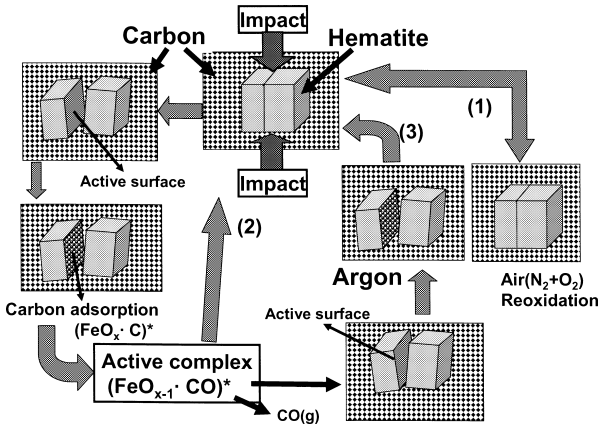

Fig. 9. Illustration of the phenomena occurring in the milling of the mixture both in the air and in the argon.

oxidation of hematite during milling under an air atmosphere might occur, simultaneously. Furthermore, this phenomenon (reduction–reoxidation) would related to the non-changed crystalline size under the air. These complicated phenomena during milling were summarized in **Fig. 9**. It was important to recognize the necessary condition that the milling of hematite and carbon should carry out in the mixture. When the milling was carried out separately and mixed together after milling, the reactivity was very low,[1] and did not reach the completion of reaction. So that it was considered that the meaning of milling in mixture would be the utilization of the active surface generated at the instance of broken.[5] If there was no oxygen gas in the atmosphere, the active surface will react with the surrounding carbon to make a active complex, which might be expressed as $(FeO_x \cdot C)^*$ and $(FeO_{x-1} \cdot CO)^*$. In the present study, it was assumed that the life time of the complex, $(FeO_{x-1} \cdot CO)^*$ was longer than that of $(FeO_x \cdot C)^*$, because the removal of oxygen from the iron oxide structure normally constituted the rate limiting step. When the complex $(FeO_{x-1} \cdot CO)^*$ was generated during milling, it could explained the CO evolution in argon atmosphere as mentioned above, because small content of the complex would proceed forward. Although the extent of the reaction of CO evolution might be small, the amount of the active complex would become large with increasing milling time. In addition, the reaction curves shown in Fig.6 were different from the samples between argon and air atmosphere. The reaction curve of sample milled under argon (Fig. 6(b)) never showed three steps, H–M, M–W and W–Fe and consisted of only one main peak. In the case of the air atmosphere, the reoxidation will soon occur and the crystalline size is almost the same as original one. Then, the distinct three steps were always kept as shown in Fig. 6(a). These processes can be illustrated in Fig. 9. The milling in air would be expressed as the path (1) in Fig. 9 and it could be expressed by (2) and (3) for the milling under inert atmosphere.

3.2. Kinetic Analysis and Rate Constant Interpretation through the Transition State Theory

3.2.1. Kinetic Analysis on the Sample Milled under Air Atmosphere: Three Steps Reduction

As shown in Fig. 6(a), reaction curves could be classified into three distinct periods, kinetic analysis have performed with following equations.[1] Actually the HM reduction was separated from other reactions and MW and WF reductions were overlapped. These reactions could be considered as the single and consecutive reaction.

$$\begin{cases} Fe_2O_3 \rightarrow Fe_3O_4: & x_H \\ Fe_3O_4 \rightarrow FeO \rightarrow Fe: & x_M, x_W \end{cases} \quad \text{.....(1)}$$

Hence, the kinetic analysis was carried out with the following equations.

$$RTG_H = -\frac{dx_H}{dt} = S_H k_H x_H = k'_H x_H \quad \text{.....(2)}$$

$$RTG_M = -\frac{dx_M}{dt} = S_M k_M x_M = k'_M x_M \quad \text{.....(3)}$$

$$RTG_W = -\frac{dx_W}{dt} = S_W k_W x_W - \left(-\frac{dx_M}{dt}\right) = k'_W x_W - k'_M x_M \quad \text{.....(4)}$$

where x (−) means the fraction of unreacted sample of respective reactions. Subscripts 'H', 'M' and 'W' mean the HM, MW and WF reductions, respectively. S (−) means the specific contact area between oxide and carbon ($S=S_p/S_0$, S_p; contacting area of the particles (cm^2), S_0; total surface area of non-milling sample (cm^2)) and k (1/s) is the reaction rate constant expressed by the Arrhenius equation, Eq. (5).

$$k_Y = A_Y \exp\left(\frac{-E_Y}{RT}\right), \quad (Y = \text{H, M and W}) \quad \text{.....(5)}$$

Where A_Y (1/s) means a frequency factor, E_Y (J/mol) means an activation energy, R (J/mol K) is the gas constant and T (K) is the absolute temperature. At first, the exact values of contact area S between the oxide and the carbon was treated as an unknown value, k' (1/s) was introduced and Eq. (6) was used in the previous analysis instead of Eq. (5).[1]

$$k'_Y = S_Y A_Y \exp\left(\frac{-E_Y}{RT}\right) = A_Y' \exp\left(\frac{-E_Y}{RT}\right), \quad (Y=\text{H, M and W}) \quad \text{.....(6)}$$

The parameter fitting to determine A'_Y and E_Y was carried out and RTG curves were recalculated.[1] The obtained rate constants for each experiments were summarized in **Table 1**(a).

The surface area of the hematite particle that was increasing with the milling time was estimated in present study. The relationships among the milling time, the surface area (cm^2) and average particle size (μm) were shown in **Fig. 10**, which were calculated by the following data: Density of hematite: $\rho_H = 5.0\,g/cm^3$, $Fe_2O_3+C = 20\,mg$, $Fe_2O_3 = 16.032\,mg$, Total volume of hematite $V_T = 3.2064 \times 10^{-3}\,cm^3$. The results were summarized in **Tables 2** and **3**, for the milling in air and for the milling in argon, respectively. The average particle size was measured based on SEM observation and the oxidation in low temperature at 550°C for separation of hematite particle from carbon mixture was adopted. According to milling, the average of par-

Table 1. Rate constants obtained by increasing milling time. (a) including the surface area, (b) except the term of surface area.

Milling time hours	(a) $k_Y(1/s) = A_Y^{'} \exp(\frac{-E_Y}{RT})$, $(Y=H, M, W), A_Y^{'} = S_Y A_Y$, E_Y (J/mol)		
	H-M	M-W	W-Fe
6	$1\times10^{5}\exp\left(\frac{-166{,}100}{RT}\right)$	$7\times10^{11}\exp\left(\frac{-357{,}100}{RT}\right)$	$1\times10^{30}\exp\left(\frac{-830{,}600}{RT}\right)$
24	$200\exp\left(\frac{-99{,}700}{RT}\right)$	$5\times10^{7}\exp\left(\frac{-249{,}200}{RT}\right)$	$1\times10^{32}\exp\left(\frac{-830{,}600}{RT}\right)$
72	$500\exp\left(\frac{-103{,}800}{RT}\right)$	$9\times10^{8}\exp\left(\frac{-265{,}800}{RT}\right)$	$6\times10^{137}\exp\left(\frac{-3322{,}300}{RT}\right)$
100	$1\times10^{4}\exp\left(\frac{-122{,}900}{RT}\right)$	$9.8\times10^{8}\exp\left(\frac{-265{,}800}{RT}\right)$	$2.5\times10^{157}\exp\left(\frac{-3737{,}50}{RT}\right)$
Milling time hours	(b) $k_Y(1/s) = A_Y \exp(\frac{-E_Y}{RT})$, E_Y (J/mol)		
	H-M	M-W	W-Fe
6	$1\times10^{4}\exp\left(\frac{-166{,}100}{RT}\right)$	$7\times10^{10}\exp\left(\frac{-357{,}100}{RT}\right)$	$1\times10^{29}\exp\left(\frac{-830{,}600}{RT}\right)$
24	$10.0\exp\left(\frac{-99{,}700}{RT}\right)$	$2.5\times10^{6}\exp\left(\frac{-249{,}200}{RT}\right)$	$5.0\times10^{30}\exp\left(\frac{-830{,}600}{RT}\right)$
72	$5.0\exp\left(\frac{-103{,}800}{RT}\right)$	$9.0\times10^{6}\exp\left(\frac{-265{,}800}{RT}\right)$	$6.0\times10^{135}\exp\left(\frac{-3322{,}300}{RT}\right)$
100	$10.0\exp\left(\frac{-122{,}900}{RT}\right)$	$9.8\times10^{5}\exp\left(\frac{-265{,}800}{RT}\right)$	$2.5\times10^{154}\exp\left(\frac{-3737{,}500}{RT}\right)$

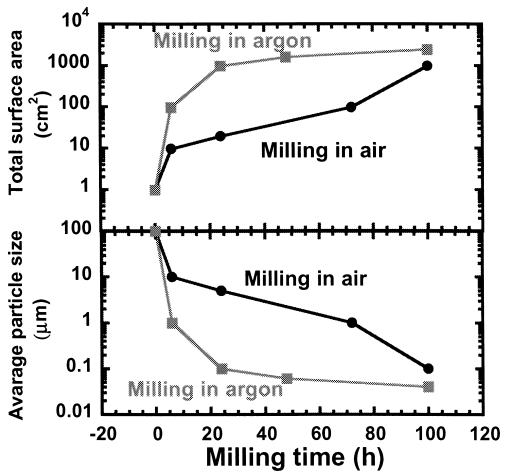

Fig. 10. Variation of average particle size and surface area with milling time.

Table 2. Average particle size and total surface area of hematite. (sintered hematite, milling in air, $V_T = 3.2064\times10^{-3}\,cm^3$)

Milling time (h)	Average particle radius r (μm)	Volume of particle, $V(cm^3)$	Number of particle, $P_N=V_T/V$	Total surface area, $S=P_N*4\,\pi r^2$	
				cm^2	$S_Y=S/S_0$
0	100	4.19×10^{-6}	765	0.962	S_0
6	10	4.19×10^{-9}	7.65×10^{5}	9.62	10
24	5	5.23×10^{-10}	6.12×10^{6}	19.2	20
72	1	4.19×10^{-12}	7.65×10^{8}	96.2	100
100	0.1	4.19×10^{-15}	7.65×10^{11}	962	1000

ticle size in argon atmosphere decreased rapidly and smaller than that of milling in air. Although the difference at 100 h was not so large, the particle size from 24 to 48 h showed a large difference between the milling in the air and in the argon. Corresponding to the smaller particle size, the

Table 3. Average particle size and total surface area of hematite. (sintered hematite, milling in argon, $V_T = 3.2064\times10^{-3}\,cm^3$)

Milling time (h)	Average particle radius r (μm)	Volume of particle, $V(cm^3)$	Number of particle, $P_N=V_T/V$	Total surface area, $S=P_N*4\,\pi r^2$	
				cm^2	$S_Y=S/S_0$
0	100	4.19×10^{-6}	765	0.962	S_0
6	1	4.19×10^{-12}	7.65×10^{8}	96.2	100
24	0.1	4.19×10^{-15}	7.65×10^{11}	962	1000
48	0.06	9.048×10^{-16}	3.54×10^{12}	1600	1664
100	0.04	2.681×10^{-16}	1.20×10^{13}	2410	2508

Table 4. Rate constants for the sample that sintered at 1 273 K for 24 h and milled in argon atmosphere.

Milling time hours	(a) $k_Y(1/s) = A_Y \exp(\frac{-E_Y}{RT})$, E_Y (J/mol)	
	H-M	M-Fe
6	$1.0\times10^{-2}\exp\left(\frac{-50{,}000}{RT}\right)$	$1\times10^{155}\exp\left(\frac{-3887{,}000}{RT}\right)$
24	$1.0\times10^{-3}\exp\left(\frac{-50{,}000}{RT}\right)$	$1.0\times10^{154}\exp\left(\frac{-3592{,}000}{RT}\right)$
48	$6.0\times10^{-4}\exp\left(\frac{-50{,}000}{RT}\right)$	$6.0\times10^{42}\exp\left(\frac{-980{,}200}{RT}\right)$
100	$2.4\times10^{-6}\exp\left(\frac{-16{,}700}{RT}\right)$	$4.0\times10^{5}\exp\left(\frac{-220{,}000}{RT}\right)$

total surface area of the sample milled in argon atmosphere was larger. Since the starting size of particle was the same, the magnification of total surface area in the argon milling at 100 h was largest ($S_Y=S/S_o=2\,508$, at 100 h).

3.2.2. Kinetic Analysis on the Sample Milled in Argon Atmosphere: Two Steps Reduction

Based on Fig. 6(b), the reaction curves could be classified into two periods, kinetic analysis have performed with following equations. The hematite reduction HM and the magnetite to metallic iron reduction, M–Fe would proceed as consecutive reaction, however, as the point of the transition was 11.5 %, both reaction could be treated as the single reaction.

$$\begin{cases} Fe_2O_3 \rightarrow Fe_3O_4: & x_H \\ Fe_3O_4 \rightarrow Fe: & x_M \end{cases} \quad \text{.....(7)}$$

Hence, the kinetic analysis was carried out with the following equations.

$$RTG_H = -\frac{dx_H}{dt} = S_H k_H x_H = k_H{}' x_H \quad \text{.....(8)}$$

$$RTG_M = -\frac{dx_M}{dt} = S_M k_M x_M = k_M{}' x_M \quad \text{.....(9)}$$

Obtained rate constants were summarized in **Table 4**, in which the term of the surface area were already eliminated using S shown in Table 3. In the present study, since it was considered that the milling conditions (time, atmosphere, crystal state of samples) were resulted in the different state of product which had completely different reactivity, the rate constants summarized in Tables 1 and 2 could be different. The reasons are showing in the following section

through the introduction of the active complexes.

In the case of argon atmosphere (as shown in Fig. 6(b)), the reduction curve of HM never showed the peak and showed almost constant value, which meant that the rate constant of HM reduction should be almost the same (very low temperature dependence).

3.3. Activated Complex Introduced by Mechanical Milling

3.3.1. Sample Milled in Air

It was found that the simple reaction of hematite with carbon was changed by the mechanical milling, which might be introduced the activated state into the mixture. The interpretation of the meaning of the obtained rate constants could be performed through the transition state theory.[6,7] According to the theory, Gibbs free energy of activation, ΔG^* can be expressed by Eq. (10).

$$\Delta G^* = \Delta H^* - \Delta S^* \cdot T \quad \text{.....(10)}$$

Where ΔH^* and ΔS^* are enthalpy of activation and entropy of activation, respectively. The rate constant of the activation can be expressed by Eq. (11).

$$k = \kappa \left(\frac{k_B T}{h} \right) \exp\left(\frac{-\Delta G^*}{RT} \right) \quad \text{.....(11)}$$

Where k_B is Boltzmann constant, κ is transmission coefficient and h is planck constant. Substitution of Eq. (10) into Eq. (11) can be obtained Eq. (12).

$$k = \kappa \left(\frac{k_B T}{h} \right) \exp\left(\frac{-\Delta H^* + \Delta S^* T}{RT} \right) = \kappa \left(\frac{k_B T}{h} \right) \exp\left(\frac{\Delta S^*}{R} \right) \exp\left(\frac{-\Delta H^*}{RT} \right) \quad \text{.....(12)}$$

On the other hand, the experimental rate constant obtained in previous study[6] is Eq. (13).

$$k_Y (1/\mathrm{s}) = A_Y \exp\left(\frac{-E_Y}{RT} \right) \quad \text{.....(13)}$$

The relationship between ΔH^* and E_Y can be expressed by Eq. (14).[6,7]

$$E_Y = \Delta H^* + (1 - \Delta n^*) \cdot RT \quad \text{.....(14)}$$

where Δn^* means the difference of moles between the reactant(s) and the activated complex, which is depending on the reaction equation including the kind of activated complex.

Although overall reaction can be expressed by Eq. (15),

$$Fe_2O_3 + 3C = 2Fe + 3CO \quad \text{.....(15)}$$

the actual reactions are considered as following consecutive reactions for the sample milled in air atmosphere.

$$3Fe_2O_3 + C = 2Fe_3O_4 + CO \quad \text{.....(16)}$$

$$Fe_3O_4 + C = 3FeO + CO \quad \text{.....(17)}$$

$$FeO + C = Fe + CO \quad \text{.....(18)}$$

These reactions were described as a removal of the one mole oxygen. The activated complexes included in Eq. (16) could be considered as follows;

$$3Fe_2O_3 + C \xrightarrow{i1} (3Fe_2O_3 \cdot C)^* \xrightarrow{i2} (2Fe_3O_4 \cdot CO)^* \xrightarrow{i3} 2Fe_3O_4^* + CO \xrightarrow{i4} 2Fe_3O_4 + CO \quad \text{.....(19)}$$

where $i2 \gg i3$ will be reasonable, because the formation and the desorption of CO gas could be the rate controlling step as mentioned above. Then Eq. (19) can be simplified as follows.

$$3Fe_2O_3 + C \xrightarrow{i1} (2Fe_3O_4 \cdot CO)^* \xrightarrow{i3} 2Fe_3O_4^* + CO \xrightarrow{i4} 2Fe_3O_4 + CO \quad \text{.....(20)}$$

Normally, the transition $Fe_3O_4^* \rightarrow Fe_3O_4$ will be very fast and it is no need to take into account. However in this study, it was assumed that the activated complex could be utilized for the next reaction, especially in the long time milling, the contact between the iron oxide and carbon maintained always until the reaction complete. So that following two cases could be considered.

$$3Fe_2O_3 + C \xrightarrow{i1} (2Fe_3O_4 \cdot CO)^* \xrightarrow{i3} 2Fe_3O_4^* + CO \quad \text{...(21)}$$

$$3Fe_2O_3 + C \xrightarrow{i1} (2Fe_3O_4 \cdot CO)^* \xrightarrow{i4} 2Fe_3O_4 + CO \quad \text{...(22)}$$

Using Eq. (21) or (22), Δn^* can be determined.

$$\Delta n^* = 1 - 4 = -3 \quad \text{.....(23)}$$

$$\Delta H_H^* = E_H + (\Delta n^* - 1) \cdot RT = E_H - 4 \cdot RT \quad \text{.....(24)}$$

Similarly, magnetite and wustite reduction were presented.

$$Fe_3O_4 + C \xrightarrow{i5} (3FeO \cdot CO)^* \xrightarrow{i6} 3FeO^* + CO \xrightarrow{i7} 3FeO + CO \quad \text{.....(25)}$$

$$FeO + C \xrightarrow{i8} (Fe \cdot CO)^* \xrightarrow{i9} Fe^* + CO \xrightarrow{i10} Fe + CO \quad \text{.....(26)}$$

For convenience, notations, H, M, W and Fe are used for Fe_2O_3, Fe_3O_4, FeO and metallic iron, respectively. The asterisk '*' means the activated state of the molecules and atom, $Fe_3O_4^*$, FeO*, Fe* and complexes $(2Fe_3O_4 \cdot CO)^*$, $(3FeO \cdot CO)^*$, $(Fe \cdot CO)^*$.

Equation (20), Eq. (25) and Eq. (26) are rewritten as follows.

$$3H + C = (2M \cdot CO)^* = 2M^* + CO = 2M + CO \quad \text{.....(20')}$$

$$M + C = (3W \cdot CO)^* = 3W^* + CO = 3W + CO \quad \text{.....(25')}$$

$$W + C = (Fe \cdot CO)^* = Fe^* + CO = Fe + CO \quad \text{.....(26')}$$

The enthalpy of activation for Eq. (25) and Eq. (26) can be calculated by Eq. (27) and Eq. (28), respectively.

$$\Delta H_M^* = E_M - 2 \cdot RT \quad \text{.....(27)}$$

$$\Delta H_W^* = E_W - 2 \cdot RT \quad \text{.....(28)}$$

Moreover, Frequency factor A_Y and the entropy of activation are expressed by Eq. (29).

Table 5. Enthalpy and entropy of activation for respective reactions for the sample milled in air.

Milling time hours	H-M		M-W		W-Fe	
	ΔS* (J/mol·K)	ΔH* (kJ/mol)	ΔS* (J/mol·K)	ΔH* (kJ/mol)	ΔS* (J/mol·K)	ΔH* (kJ/mol)
6	1132K		1310 K		1344 K	
	-179.2	128.5	-49.5	335.4	+297.5	808.2
24	1090 K		1255 K		1281 K	
	-236.3	63.5	-134.3	228.3	+330.3	808.2
72	1029 K		1207 K		1236 K	
	-241.6	69.6	-123.3	245.7	**+1178**	**3301**
100	983 K		1203 K		1214 K	
	-235.4	90.3	-141.7	245.8	**+1453**	**3717**

$$A_Y = \kappa \left(\frac{k_B T}{h}\right) \exp\left(\frac{\Delta S^*}{R}\right) \quad \text{.....(29)}$$

Using experimental A_Y and E_Y shown in Table 1(b), which were already eliminated the effect of surface area of hematite, the enthalpy ΔH^* and the entropy ΔS^* of activation were evaluated and summarized in **Table 5**. The temperatures for the enthalpy and entropy were adopted the peak temperatures of the respective reaction curves, which were obtained in previous study,[1] (*cf.* Table 2 in the reference[3]). In this study, the value of κ in Eq. (29) was assumed as unity.

(1) Feature of Hematite (H–M) and Magnetite (M–Fe) Reduction

The inherent image of the transition state can be understood through the entropy of activation, ΔS^*. The negative value of ΔS^* means the vanishing of the freedom for the vibrations of the rotation and the translation from reactant to complex.[7] The H–M and M–W reduction are corresponding to this situation. Especially in present experiment, the 6 h milling time and the longer ones (24 h, 72 h and 100 h) showed different situation. It was considered that the activated complex did not constructed completely in the case of 6 h milling, which could understood by the change of activation energy (the value of activation energy decreased from 6 to 24 h, then, increased monotonously from 24 to 100 h). ΔS^* of H–M reduction from 24 to 100 h almost the same (-240 J/mol·K), however, it decreased from 6 h (-179 J/mol·K) to 24 h (-236 J/mol·K) which meant the complex, (2M·CO)* lost the freedom of some vibration from 6 h milling to 24 h milling.

The M–W reduction showed almost the same tendency as the H–M reduction. These explanations on the nature of the activated complex would also discussed through the partition function as follows:

Equation (11) can be rewritten by using the partition function.[6,7]

$$k = \kappa \left(\frac{k_B T}{h}\right)\left(\frac{F_{MCO}^*}{F_H F_C}\right) \exp\left(\frac{-E_0}{RT}\right) \quad \text{.....(30)}$$

Where F^*_{MCO}, F_H, F_C are the partition function for the complex, hematite and carbon.

If the reaction was simplified to $A+BC \rightarrow A\cdots B\cdots C \rightarrow AB+C$, each partition functions can be expressed by Eqs. (31) and (32).[6,7]

$$F^* = g^* \frac{(2\pi m_* k_B T)^{3/2}}{h^3} \frac{8\pi I_* k_B T}{\sigma_* h^2} \prod \left(1-\exp\left(\frac{-h\nu_*}{k_B T}\right)\right)^{-1} \quad \text{.....(31)}$$

$$F_A \cdot F_{BC} = g_1 \frac{(2\pi m_1 k_B T)^{3/2}}{h^3} g_2 \frac{(2\pi m_2 k_B T)^{3/2}}{h^3} \frac{8\pi I_2 k_B T}{\sigma_2 h^2} \times \left(1-\exp\left(\frac{-h\nu_2}{k_B T}\right)\right)^{-1} \quad \text{.....(32)}$$

The term corresponding to the entropy of activation, $F^*/(F_A \cdot F_{BC})$ would decrease with the decrease of F^* because of losing of some vibration mode, $\prod(1-\exp(-h\nu_*/k_B T))^{-1}$, which would correspond to the change of ΔS^* from 6 to 24 h.

Moreover, as this term related to the temperature dependence, the activation energy E_Y would also decrease with the term of $\prod(1-\exp(-h\nu_*/k_B T))^{-1}\exp(-E_0/RT)$.

(2) Feature of Wustite (W–Fe) Reduction

On the other hand, wustite (W–Fe) reduction showed entirely different behavior. The values of the entropy of activation, ΔS^* was positive and quite large value (Table 5). Furthermore, the enthalpy of activation, ΔH^* was extremely high according to the milling time. The positive value of ΔS^* means that the activated complex has larger entropy than that of reactant. Moreover, a loose bonded complex has larger entropy than that of rigid bonded complex.[7] From this point of view, the positive and extremely high value of ΔS^* meant the complex of (Fe·CO)* having a loose bond, which corresponded to the high reaction rate.

3.3.2. Sample Milled in Argon

Similarly to the analysis of activation complex on the sample milled in the air, the rate constants obtained from the reaction of sample milled in the argon atmosphere were analyzed as follows.

Hematite reaction was the same as Eq. (2). However, Magnetite reduction M–Fe can be expressed as Eq. (33).

$$1/4\,Fe_3O_4 + C = 3/4\,Fe + CO \quad \text{.....(33)}$$

And active complex can be expressed by Eq. (34).

$$\frac{1}{4}Fe_3O_4 + C \xrightarrow{i1} \left(\frac{3}{4}Fe\cdot CO\right)^* \xrightarrow{i3} \frac{3}{4}Fe^* + CO \xrightarrow{i4} \frac{3}{4}Fe + CO \quad \text{.....(34)}$$

The difference of mole between the complex and the reactants is

$$\Delta n^* = 1 - \frac{5}{4} = -\frac{1}{4} \quad \text{.....(35)}$$

Then the enthalpy of activation can be calculated by Eq. (36).

$$\Delta H_M^* = E_M + (\Delta n^* - 1)\cdot RT = E_M - \frac{5}{4}\cdot RT \quad \text{.....(36)}$$

The enthalpy (ΔH^*) and entropy (ΔS^*) of activation were

Table 6. Enthalpy and entropy of activation for respective reactions for the sample milled in argon.

Milling time hours	H-M $\Delta H_M^* = E_M - 4 \cdot RT$		M-W $\Delta H_M^* = E_M - \frac{5}{4} \cdot RT$	
	ΔS* (J/mol·K)	ΔH* (kJ/mol)	ΔS* (J/mol·K)	ΔH* (kJ/mol)
6	500K		1285K	
	-287.5	33.37	+2710.2	3873.6
24	500K		1173 K	
	-306.6	33.37	+2691.8	3579.8
48	500K		1063K	
	-310.9	33.37	+563.45	969.15
100	500 K		982K	
	-356.8	0.072	-147.58	209.79

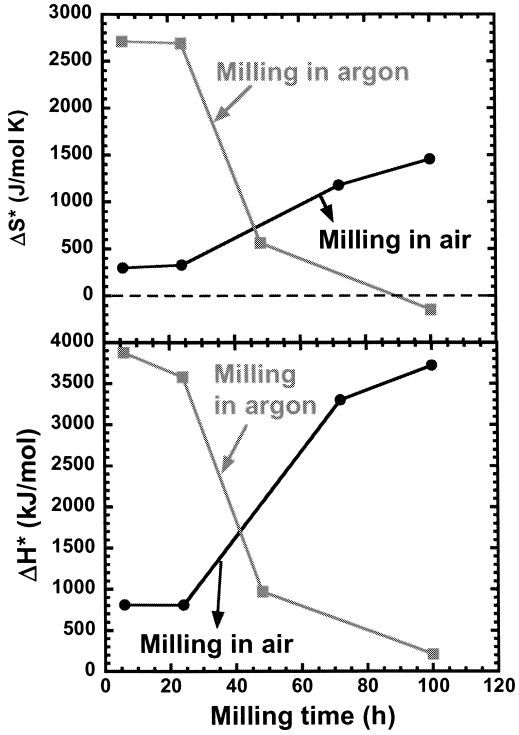

Fig. 11. Comparison of enthalpy ΔH^* and entropy ΔS^* of activation obtained in the different milling conditions.

estimated by Eqs. (36) and (29), respectively. The obtained values are shown in **Table 6** and plotted against the milling time in **Fig. 11** (W–Fe reduction in air milling, M–Fe reduction in argon milling). It was found that ΔH^* and ΔS^* varied same way with milling time. When ΔS^* increased (decreased) with milling time, ΔH^* also increased (decreased). However, the way of variation between the milling in the air and in the argon was opposite, which meant that completely different feature (transition state) of product were assigned by milling between two conditions. As mentioned above, the positive and extremely high value of ΔS^* meant the complex of $(Fe \cdot CO)^*$ having a loose bond owing to the milling in air. Contrary to the milling in air, the sample milled in argon atmosphere gave the decreasing tendency of the entropy of activation, ΔS^*. In the case of milling in air, the active complex having a loose bond was generated during milling. On the other hand, in argon atmosphere, it would be the vanishing process of some vibration mode for the bondings. So that the milling in argon makes the active complex having relatively tight bond close to the state

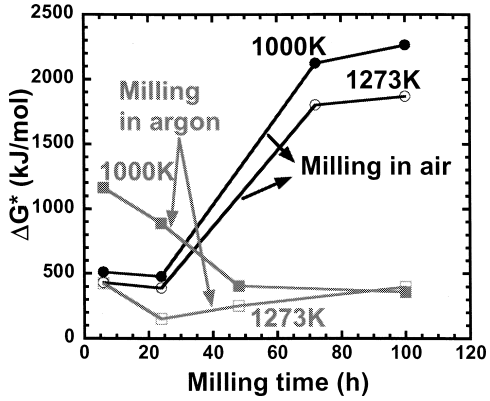

Fig. 12. Comparison of Gibbs free energy ΔG^* of activation obtained in the different milling conditions.

of the product. The complex would have a different structure from the reactant loosing some vibration mode. In other words, the complex made in argon atmosphere would have a structure similarly to the product one. Therefore, the reactivity of milling sample was extremely higher than that in the air.

Gibbs free energy of activation, ΔG^* was evaluated at 1 000 and 1 273 K using ΔH^* and ΔS^* obtained, as shown in **Fig. 12**. ΔG^* for milled in the air has extremely high value in longer milling time and it decreased with increasing temperature from 1 000 to 1 273 K. Corresponding to this, ΔG^* from the sample milled in the argon atmosphere decreased with the increasing milling time. Moreover, it decreased largely from 1 000 to 1 273 K, which meant the reaction needed the higher energy to proceed in the lower temperature.

4. Conclusions

Milling of hematite and graphite mixture was carried out both in the air and in the argon. Rate constants for the reactions were obtained by kinetic analysis. The enthalpy ΔH^* and entropy ΔS^* of activation were estimated on the basis of transition state theory. The interpretation of ΔS^* and ΔH^* was performed to explain the effect of milling on the reactivity related to the milling conditions. The results obtained are as follows.

(1) The temperature of peak of reaction curve decreased with increasing milling time. The reactivity of the sample milled in the argon atmosphere showed higher reactivity than that milled in the air.

(2) The reaction consisted of three steps (HM, MW and WFe reduction) for the sample milled in the air, while there were two reaction steps (HM and MFe reduction) existed in the reaction of sample milled in the argon.

(3) From the results of XRD, the crystalline size in the sample milled in air showed almost constant size, while the crystalline size milled in argon decreased. Taking into account of the CO gas evolution during milling, it was considered the reduction reaction occurred. Especially, reoxidation should occur during the milling in the air atmosphere. The difference of crystal state after milling should result in the quite different reactivity through the active complex.

(4) The enthalpy ΔH^* and entropy ΔS^* of activation were obtained from experimental rate constants on the basis

of transition state theory. The variation of ΔH^* and ΔS^* with milling time showed opposite tendency between the sample milled in the air and in the argon.

(5) It was considered that the active complex having loose bonding would form during milling in the air atmosphere. On the other hand, the active complex having a structure closed to the product (metallic iron) might form.

Acknowledgement

The present study has been carried out in the research group of 'Project for the innovational ironmaking reaction in new blast furnace at half energy consumption and minimum environmental influences' supported by Special Coordination Founds of the Science and Technology Agency of the Japanese Government. The authors would like to express great appreciation to the member of research group for the valuable discussions.

REFERENCES

1) J. Vahdati Khaki, Y. Kashiwaya, K. Ishii and H. Suzuki: *ISIJ Int.*, **42** (2002), 13.
2) Y. Kashiwaya, M. Kanbe and K. Ishii: *ISIJ Int.*, **41** (2001), 818.
3) Y. Kashiwaya and K.Ishii: *ISIJ Int.*, **31** (1991), 440.
4) Y. Kashiwaya, H. Suzuki and K. Ishii: *ISIJ Int.*, **44** (2004), 1970.
5) Y. Kashiwaya, R. Suzuki and K. Ishii: *ISIJ Int.*, **44** (2004), 1975.
6) S. Glasstone, K. J. Laidler and H. Eyring: The Theory of Rate Processes, McGraw-Hill, New York and London, (1941), 146.
7) W. J. Moore: Physical Chemistry 4th Ed., Tokyo Kagaku Dojin, Tokyo, (1978), 387.